Investigation of the Copper Gettering Mechanism of Oxide Precipitates in Silicon

G. Kissinger,[a,*,z] D. Kot,[a,*] M. Klingsporn,[a] M. A. Schubert,[a] A. Sattler,[b] and T. Müller[b]

[a]IHP, 15236 Frankfurt (Oder), Germany
[b]Siltronic AG, 81737 München, Germany

One of the reasons why the principal gettering mechanism of copper at oxide precipitates is not yet clarified is that it was not possible to identify the presence and measure the copper concentration in the vicinity of oxide precipitates. To overcome the problem we used a 14.5 nm thick thermal oxide layer as a model system for an oxide precipitate to localize the place where the copper is collected. We also analyzed a plate-like oxide precipitate by EDX and EELS and compared the results with the analysis carried out on the oxide layer. It is demonstrated that both the interface between the oxide precipitate being SiO_2 and the silicon matrix and the interface between the thermal oxide and silicon consist of a 2–3 nm thick SiO layer. As the results of these experiments also show that copper segregates at the SiO interface layer of the thermal oxide it is concluded that gettering of copper by oxide precipitates is based on segregation of copper to the SiO interface layer.
 [DOI: 10.1149/2.0151509jss]

Manuscript submitted July 7, 2015; revised manuscript received August 6, 2015. Published August 14, 2015.

The precipitation of interstitial oxygen in silicon wafers is a research issue of ongoing interest since decades because it impacts device manufacturing in several ways. Among others, oxide precipitates are utilized for internal gettering of metallic impurities in the front end and back end of electronic device manufacturing.[1–3] Although the effect of internal gettering is known since the eighties the mechanism of gettering is still under dispute.

In this work, we focus on gettering of copper impurities. Copper is one of the most significant and harmful metal contaminants to take care of in electronic device processing. It is known to degrade the device performance by causing junction leakage currents and early breakdown of gate oxides.[4,5] Copper is also known to increase the light induced degradation of solar cells.[6]

Dislocations and stacking faults are well known as efficient gettering sites for copper[7] but according to Istratov et al. the oxide precipitates are rather weak gettering sites.[8,9] However, it was established that oxide precipitates without accompanying secondary defects can getter copper impurities.[10,11] Väinölä et al. showed that under high-intensity illumination, oxide precipitates provided effective heterogeneous nucleation sites for copper.[12] Sueoka demonstrated that the getter efficiency of oxide precipitates depends on their size and density and he defined a critical size versus density ratio.[13] Hölzl et al. found that the total inner surface is important for the getter efficiency and they defined a critical normalized inner surface for efficient gettering of copper.[14] Kot et al. showed that Hölzl's threshold shifts to lower values if the oxide precipitates have generated secondary defects.[15] Moreover, they found that gettering of copper impurities at dislocations is stronger in samples contaminated with high copper concentration where further growth of copper silicide precipitates occurs by a repeated nucleation process on climbing edge dislocations. In case of low copper contamination, gettering at dislocations was less important and oxide precipitates became the main getter sink for copper.

Several mechanisms for copper gettering were proposed. The copper atoms can be trapped inside of oxide precipitates, in the region of strained Si around precipitates,[16] at the surface of the oxide precipitates,[14] or even Si interstitials emitted from oxide precipitates could be possible getter sites for copper contaminations.[17,18] Sueoka et al. calculated the total energy change for Cu in strain free Si attached to the various getter sites.[19] They found for single Cu atoms that from the energetic point of view trapping at the surface of oxide precipitates or the interaction with emitted silicon interstitials are possible mechanisms for Cu gettering. Bai et al. demonstrated that copper is gettered to the Si/SiO_2 interface during thermal growth of a silicon oxide layer.[20]

Strained Si would also be a possible getter site but only if the silicon lattice is under tensile strain.[16] The molecular volume of the oxide precipitate is larger than the molecular volume of Si. Therefore, the Si lattice surrounding the precipitate is compressively strained. However, it was found for plate-like precipitates that the strain along the direction parallel to the precipitate is tensile in contrast to the strain along the direction normal to plate-like precipitate which is compressive.[21] This means that at the edges of plate-like oxide precipitates the silicon lattice is under tensile strain. Thus, plate-like precipitates could provide getter sites for metal impurities.

In summary, it can be said that the principal getter mechanism at oxide precipitates is not yet clarified. One of the main reasons is that it is not possible to measure the copper concentration in the vicinity of oxide precipitates because the sensitivity of techniques with suitable spatial resolution, like EDX, is much too low. Therefore, the objective of this work was to use a 14.5 nm thick oxide layer as a model system on which to detect by time of flight secondary ion mass spectrometry (ToF-SIMS) where copper from a suitably generated supersaturated solution is collected. We also analyzed a plate-like oxide precipitate by energy dispersive X-ray (EDX) investigation and electron energy loss spectrometry (EELS) and compared the results with a similar analysis of the oxide layer. These investigations enabled us to draw conclusions about the nature of the gettering sink of copper at oxide precipitates.

Experimental

For the experiments, samples of 1.3 cm × 1.0 cm size were cut from a Czochralski silicon wafer with an oxide layer of 14.5 nm thickness. The oxide layer was obtained by dry oxidation at 900°C with HCl added. The samples were contaminated afterwards with copper by letting a drop of an aqueous solution containing 1000 ppm of copper dry on the surface. In this way, we deposited copper in the range of 10^{15} cm^{-2} on the samples. During a drive-in anneal at 500°C for 30 min in nitrogen the copper diffused into the silicon samples. Then, the depth profile of the copper distribution was analyzed after the drive-in anneal and again after 70 days of storage by ToF-SIMS using oxygen (500 eV) and cesium (1 keV) sputter sources on an area of 300 μm × 300 μm. The analyzing source was a bismuth source (25 keV) analyzing an area of 100 μm × 100 μm.

Interface details of the thermal oxide were also carefully studied to infer the mechanism of copper gettering at a thermal oxide layer,

*Electrochemical Society Active Member.
zE-mail: gkissinger@ihp-microelectronics.com

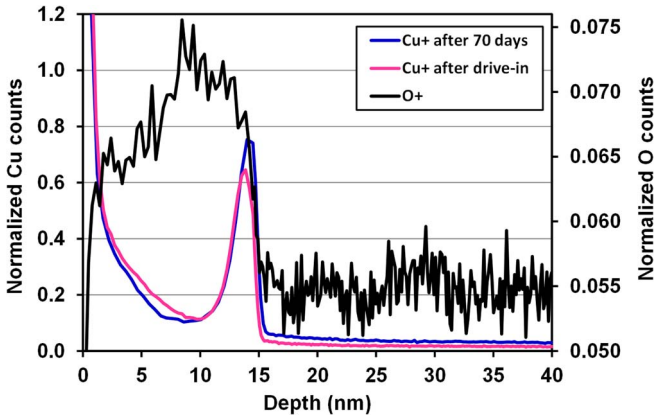

Figure 1. Depth profile of copper and oxygen in an oxidized silicon wafer intentionally contaminated with copper analyzed by ToF-SIMS after drive-in at 500°C using an oxygen sputter source. The copper profile was measured again after 70 days. The counts were normalized with respect to the counts of ^{30}Si.

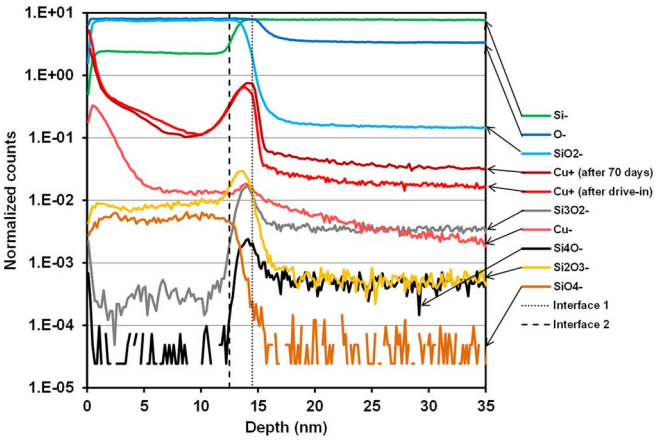

Figure 2. Depth profile of copper, silicon, and oxygen containing ions in an oxidized silicon wafer intentionally contaminated with copper analyzed by ToF-SIMS after drive-in at 500°C followed by 70 days of storage using a cesium sputter source. The graph also contains the depth profiles of copper measured by ToF-SIMS using an oxygen sputter source after drive-in at 500°C and after 70 days of storage. The counts were normalized with respect to the counts of ^{30}Si.

in the preliminary hypothesis that the interface of our model system is structurally and chemically similar to that of an oxygen precipitate.

To confirm the hypothesis the interface properties of oxide precipitates were investigated in a sample obtained from a Czochralski silicon wafer after a thermal treatment consisting of a rapid thermal anneal (RTA) at 1250°C for 30 s in argon atmosphere containing 1000 ppm of oxygen followed by a two-step furnace anneal at 800°C for 8 h and 1000°C for 16 h in nitrogen. A scanning transmission electron microscope (STEM) FEI TECNAI Osiris equipped with tools for EDX analysis and EELS was used to analyze the interface and composition of a plate-like precipitate located at a very thin place of the foil prepared from the sample by ion milling. The results were compared with a similar investigation of the samples of the oxidized silicon wafer.

Results

Investigation of a thermal oxide layer.— Figure 1 shows the depth profile of copper and oxygen in the oxidized silicon wafer analyzed by ToF-SIMS after drive-in at 500°C using the oxygen sputter source which has a high sensitivity for copper profiles. It can be seen that the copper concentration is increased in the part of the oxide layer which is close to the silicon substrate. The copper profile remained nearly the same after 70 days of storage.

In order to investigate the oxide layer with a higher sensitivity the cesium sputter source was used and the sample stored for 70 days was analyzed again by ToF-SIMS. The depth profiles of different Si_xO_y ions can be found in Fig. 2. Sputtering of copper is easier in the positive ion mode that means if an oxygen sputter source is used. Therefore, the copper profiles measured with the oxygen sputter source are also shown in Fig. 2. Comparing the depth profiles of the different ions analyzed it becomes clear that in the same region where the copper concentration is enhanced also the Si_xO_y species with a high x/y ratio are enhanced while the species with the lowest x/y ratio are enhanced in the central region of the oxide layer. This indicates that the composition of the oxide layer close to the silicon substrate is that of a suboxide. These results are in agreement with the results of Fukuda et al. who used EELS to analyze the interface between the silicon substrate and a 5 nm oxide layer.[22] We have drawn two interface lines in Fig. 2. Interface 1 is located at the depth where Si^- starts to decrease and Interface 2 is located at the depth where SiO_2^- starts to decrease. The region between the two interfaces is 2 nm wide. If we look at the peaks in the Cu+ depth profiles, the layer width of enhanced copper concentration is rather 3 nm.

We investigated the layer with enhanced copper concentration by STEM in more detail and searched for copper silicide precipitates but no precipitates were found. This means that the enriched copper is dissolved in the interface layer.

In order to get more detailed information about the region where the copper concentration is enhanced we also used EELS and took several EELS spectra in the interface region between the oxide and silicon substrate. We investigated the plasmon peaks in the low loss energy range. These peaks exhibit characteristic shapes and energy losses for Si, SiO, and SiO_2.[23] The plasmon peak of SiO_2 has a maximum at about 23 eV and the maximum of the Si plasmon peak can be found at about 16.7 eV. By EELS investigation of pure SiO, we found that the maximum of the plasmon peak of SiO is located at about 19 eV.

Figure 3 shows the EELS spectra of the plasmon loss taken every 0.4 nm along a line across the interface between the 14.5 nm thick

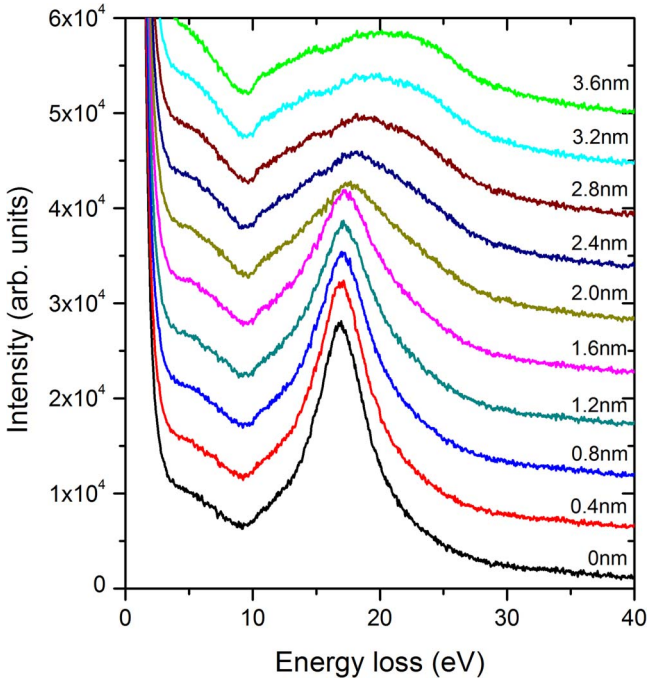

Figure 3. EELS spectra of the plasmon loss recorded every 0.4 nm along a line across the interface between a 14.5 nm thick thermal oxide and the silicon substrate.

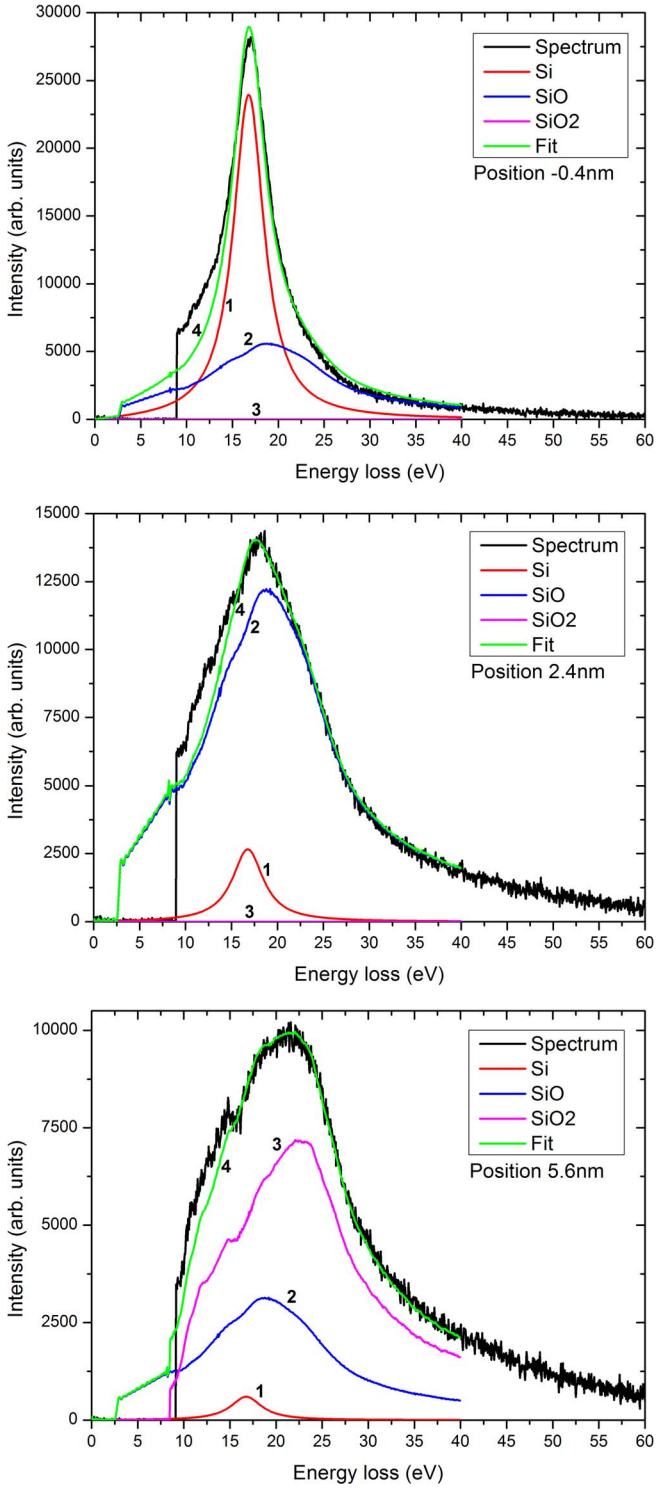

Figure 4. Deconvoluted (4) EELS spectra taken at positions −0.4 nm in the silicon substrate (top graph), 2.4 nm (middle graph), and 5.6 nm in the SiO_2 layer (bottom graph). The plasmon peaks of Si (1), SiO (2), and SiO_2 (3) were fitted to the spectrum. Before doing this, the zero loss peak of each spectrum was used to extract the single scattering distribution by Fourier logarithm deconvolution.

thermal oxide and the silicon substrate. The EELS spectra shown in Fig. 3 belong to the positions where changes in the spectra were observed. Before and after these positions the spectra did not change anymore. Position 0 was defined as the point on the interface where the

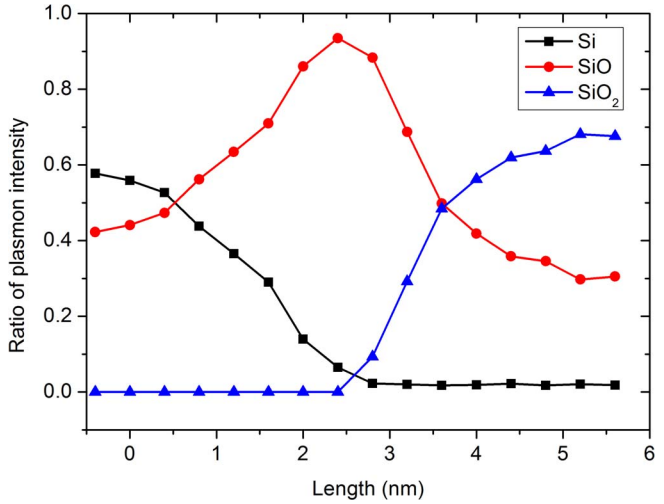

Figure 5. Ratio of the plasmon intensity of Si, SiO, and SiO_2 plotted as a function of the position on a line across the interface between oxide layer and silicon substrate. Position 0 is defined as the point of the interface where the contrast changes from black to white in the STEM HAADF image.

contrast changes from white to black in the STEM high-angle annular dark-field (HAADF) image. Comparing the EELS spectra in Fig. 3 it can be seen that the maximum shifts to higher energy with increasing distance of the position. Because we know the plasmon peaks of Si, SiO, and SiO_2, we can deconvolute the spectra in order to determine the ratio between the plasmon intensities of the three components. Before doing this, the zero loss peak of each spectrum was extracted and used to calculate the single scattering distribution by Fourier logarithm deconvolution.[24,25] Examples of the deconvoluted spectra at characteristic positions can be found in Fig. 4. The spectrum in Fig. 4 top was taken on the silicon substrate and the main contribution comes from the silicon plasmons. In the spectrum of the SiO_2 layer shown in Fig. 4 bottom, the main contribution comes from the SiO_2 plasmons. At an intermediate position (Fig. 4 middle) the SiO plasmons are dominating. In the region of both the silicon substrate and of the SiO_2 layer also a small amount of SiO was found. This is due to a very thin native oxide layer on the thin foil investigated by STEM which contributes to the EELS spectra.

The ratio of the plasmon intensity of the different components plotted for the different positions can be found in Fig. 5. It is clearly seen that between the silicon substrate and the SiO_2 layer an interface layer exists which consists of SiO. The thickness of this region lies in the range of 2–3 nm.

Investigation of an oxide precipitate.— The interface of a plate-like oxide precipitate is shown in the bright field STEM image in Fig. 6 left. The EDX images of oxygen and silicon in Fig. 6 middle and Fig. 6 right, respectively, confirm that it is an oxide precipitate. The main plane of the platelet is located perpendicular to the thin foil investigated by STEM. The side length of the precipitate amounts 208 nm. From the EELS spectra described later we know that it completely penetrates the sample foil which has a thickness of about 30 nm at this place. The foil thickness was measured by the EELS log-ratio technique[26] which is integrated in the software "DigitalMicrograph" from Gatan.

The HAADF image in Fig. 7 shows the precipitate and arrows mark the line along which EELS spectra were recorded every 0.57 nm. In Fig. 8, the EELS spectra can be found. Before and after the positions of the spectra shown here the spectra did not change anymore. The spectra look very similar to the spectra of the oxide layer in Fig. 3. We can also recognize a similar shift of the maximum of the plasmon peaks to higher energies with increasing distance of the position. Here, the position 0 was also defined as the point on the interface where the contrast changes from white to black in the STEM HAADF image.

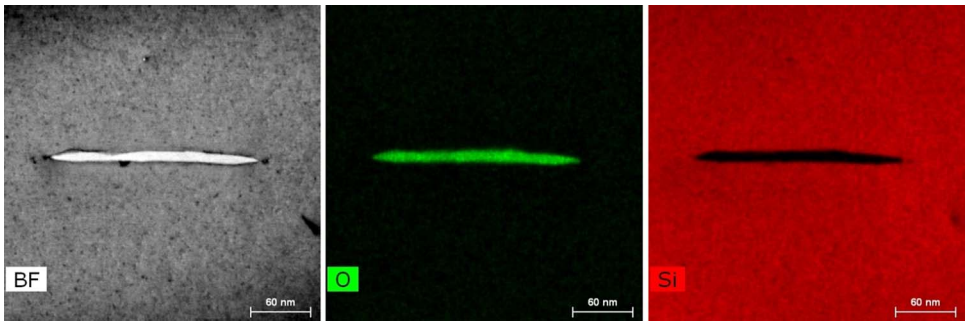

Figure 6. Bright field STEM image of a plate-like oxide precipitate (left) and the corresponding EDX images of oxygen (center) and silicon (right).

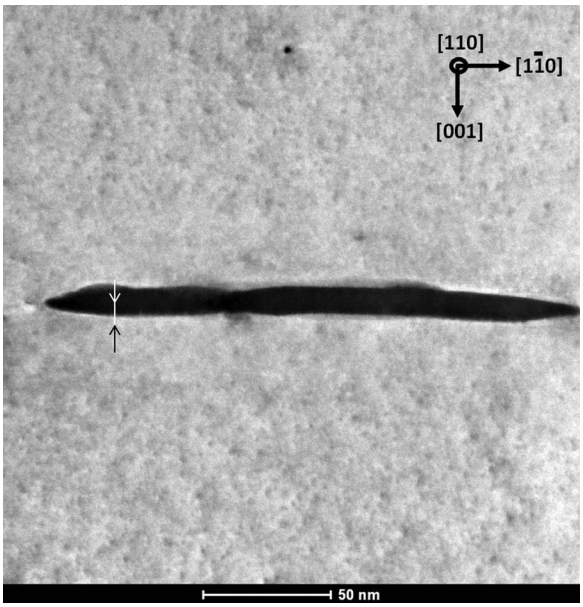

Figure 7. HAADF image of a plate-like oxide precipitate indicating the line along which EELS spectra were recorded.

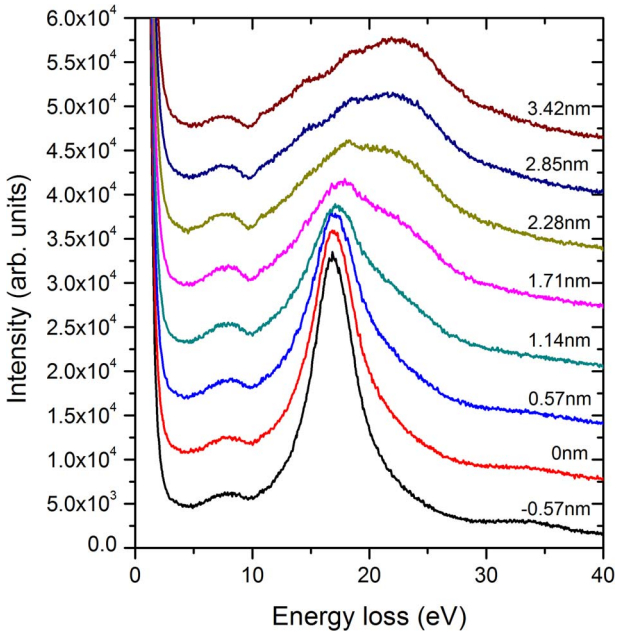

Figure 8. EELS spectra of the plasmon loss recorded every 0.57 nm along a line across the interface between a plate-like oxide precipitate and the surrounding silicon matrix.

We can confirm here also our earlier published result that the oxide precipitate itself consists of SiO_2[27] because the EELS spectrum at position 3.42 nm located in the precipitate is a typical EELS spectrum of SiO_2.[23]

We deconvoluted the EELS spectra in the same way as in the case of the spectra of the oxide layer. Examples of the deconvoluted spectra at characteristic positions can be seen in Fig. 9. The spectrum of the silicon matrix in Fig. 9 top exhibits a dominating Si plasmon peak and in the spectrum of the oxide precipitate in Fig. 9 bottom nearly only SiO_2 plasmons were detected. At the intermediate position in Fig. 9 middle, a large SiO plasmon peak was found similar to the intermediate position of the oxide layer. The resulting ratios of the plasmon intensities for the analyzed positions can be found in Fig. 10. The results are very similar to the results of the oxide layer. We also found a SiO interface layer with a thickness in the range of 2–3 nm.

An investigation of the copper distribution at oxide precipitates is not possible because ToF-SIMS is not able to analyze such small regions, although the detection limit of this method would be low enough. EDX would be able to analyze the composition in such small regions however the detection limit is several orders of magnitude higher than the copper concentration.

Discussion

Yamazaki et al. also analyzed a Si/SiO_2 interface and they found that it is constructed from three components Si, SiO_2, and an interface plasmon state.[23] Their so-called interface plasmon has the highest intensity at the interface between Si and SiO_2. The shape and location of this plasmon peak corresponds very well to our SiO plasmon peak. The existence of a SiO interface layer at the interface between an 140 nm thick SiO_2 layer and a (111) silicon substrate was also demonstrated by Moreau et al.[28] Couillard studied gate stacks with 2 nm and 10 nm thick oxide layers by detailed EELS investigation.[29] In their spectra a similar shift of the plasmon peaks as in our spectra was observed. In summary, our results are well in agreement with other works and the existence of an SiO interface layer between an SiO_2 layer and a silicon substrate seems to be well established.

In case of oxide precipitates the stoichiometry is under dispute since decades. Based on the analysis of the growth kinetics, Vanhellemont proposed that their composition is rather that of SiO.[30] This was confirmed by FTIR studies by DeGryse et al.[31] and TEM investigations of Nicolai et al.[32] However, Borghesi et al. determined the composition of plate-like precipitates by FTIR to be $SiO_{1.8}$.[33] Meduňa et al. also found the x of the SiO_x precipitates in the range between 1.8 and 2 by FTIR.[34] Kot et al. found that the absorption bands attributed to plate-like and octahedral precipitates can be both simulated by the dielectric function of amorphous SiO_2.[27] Our present investigation has shown that the plate-like precipitate investigated consists of SiO_2 thus confirming the results of the latter works.

The interface between the silicon matrix and the oxide precipitate was investigated for the first time in this work. It was shown that it is similar to the interface between a thermal oxide layer and the silicon substrate and that it consists of a 2–3 nm thick SiO layer.

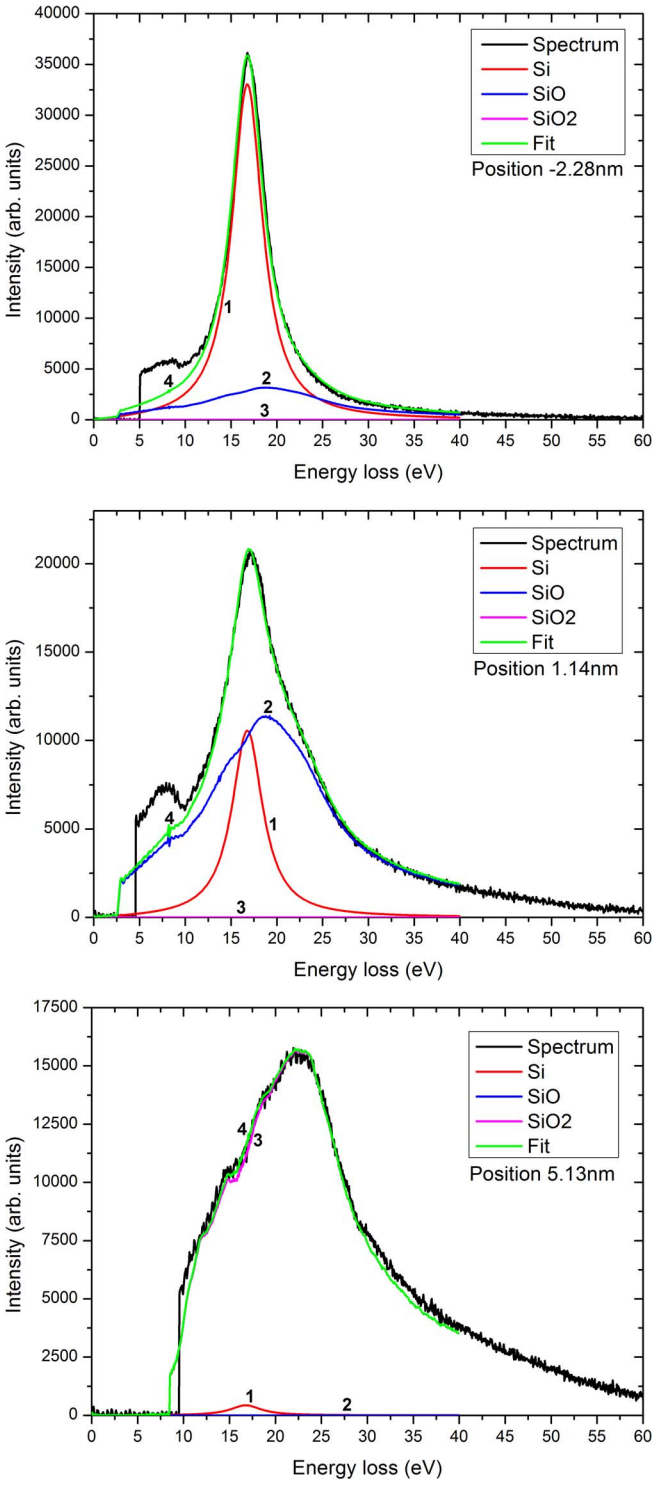

Figure 9. Deconvoluted (4) EELS spectra taken at positions −2.28 nm in the silicon matrix (top graph), 1.14 nm (middle graph), and 5.13 nm in the oxide precipitate (bottom graph). The plasmon peaks of Si (1), SiO (2), and SiO_2 (3) were fitted to the spectrum. Before doing this, the zero loss peak of each spectrum was used to extract the single scattering distribution by Fourier logarithm deconvolution.

We demonstrated that copper segregates to this SiO interface layer in case of the thermal oxide layer. Based on these results it seems reasonable to conclude that gettering of copper by oxide precipitates is based on the same mechanism, i.e. what means that gettering by oxide precipitates is by a segregation type of gettering.

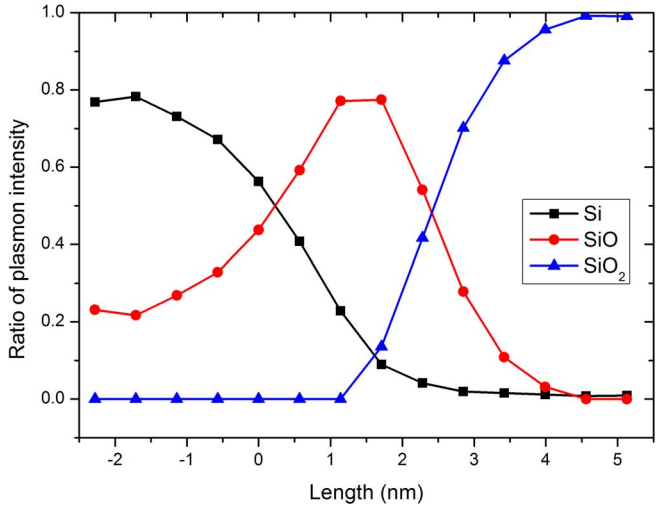

Figure 10. Ratio of the plasmon intensity of Si, SiO, and SiO_2 plotted as a function of the position on a line across the interface between an oxide precipitate and the surrounding silicon matrix. Position 0 is defined as the point of the interface where the contrast changes from black to white in the STEM HAADF image.

Isomae et al. found that the concentration of copper which is gettered is increasing with increasing copper contamination[35] which is in agreement with segregation type gettering. In contrast to relaxation type gettering which is based on copper silicide precipitation and thus requires supersaturated copper, segregation type gettering would work at any copper concentration.[36] In another work, we demonstrated that oxide precipitates can getter copper, which was driven-in at only 300°C, very efficiently.[37] It is very unlikely that this is based on nucleation of copper silicide precipitates because of the low temperature and the low supersaturation. Segregation effects become more pronounced with decreasing temperature and segregation gettering would still work. At 300°C, the diffusivity of copper is still high enough to reach the gettering sinks.[38]

Conclusions

One of the reasons why the principal gettering mechanism of copper at oxide precipitates was not yet clarified depends on the sensitivity of techniques with suitable spatial resolution, like EDX, that is much too low to allow the measurement of the copper concentration in the vicinity of oxide precipitates. In addition, the nature of the interface between oxygen precipitates and the silicon matrix was an experimental unknown. Therefore, we investigated both the interface between a plate-like oxide precipitate consisting of SiO_2 and the silicon matrix and the interface between a 14.5 nm thick thermal oxide and the silicon substrate. It was demonstrated that in both cases the interface consists of a 2–3 nm thick SiO layer.

Copper contamination experiments have shown that copper segregates to the SiO interface layer of the thermal oxide. From this behavior and the similar nature of the interface it is concluded that gettering of copper by oxide precipitates is based on segregation of copper to the SiO interface layer.

References

1. T. Y. Tan, E. E. Gardner, and W. K. Tice, *Appl. Phys. Lett.*, **30**, 175 (1977).
2. G. A. Rozgonyi and C. W. Pearce, *Appl. Phys. Lett.*, **32**, 747 (1978).
3. J. H. An, J. S. Kim, J. Y. Kim, K. S. Lee, H. B. Kang, B. S. Moon, S. H. Lee, Y. Shin, S. M. Hwang, and H. Y. Park, *ECS Transactions*, **50**, 319 (2012).
4. K. Matsushita, H. Yamamoto, and Y. Mashiko, *Jpn. J. Appl. Phys.*, **41**(Part 1), 5900 (2002).
5. R. Hölzl, A. Huber, L. Fabry, K.-J. Range, and M. Blietz, *Appl. Phys. A: Mater. Sci. Process.*, **72**, 351 (2001).
6. H. Savin, M. Yli-Koski, and A. Haarahiltunen, *Appl. Phys. Lett*, **95**, 152111 (2009).
7. B. Shen, T. Sekiguchi, J. Jablonski, and K. Sumino, *J. Appl. Phys.*, **76**, 4540 (1994).

8. A. A. Istratov, R. Sachdeva, C. Flink, S. Balasubramabian, and E. R. Weber, *Solid State Phenomena*, **82–84**, 323 (2002).
9. A. A. Istratov, C. Flink, H. Hielsmair, E. R. Weber, and T. Heiser, *Phys. Rev. Lett.*, **81**, 1243 (1998).
10. M. Seacrist, M. Stinson, J. Libbert, R. Standley, and J. Bins, *Proc. Semiconductor Silicon 2002*, ed. by H. R. Huff, L. Fabry, and S. Kishino, in: *Electrochem. Soc. Proc.* **2002-2**, 638 (2002).
11. R. J. Falster, G. R. Fisher, and G. Ferrero, *Appl. Phys. Lett.*, **59**, 809 (1991).
12. H. Väinölä, M. Yli-Koski, A. Haarahiltunen, and J. Sinkkonen, *J. Electrochem. Soc.*, **150**, G790 (2003).
13. K. Sueoka, S. Sadamitsu, Y. Koike, T. Kihara, and H. Katahama, *J. Electrochem. Soc.*, **147**, 3074 (2000).
14. R. Hölzl, M. Blietz, L. Fabry, and R. Schmolke, *Proc. Semiconductor Silicon 2002*, ed. by H. R. Huff, L. Fabry, and S. Kishino, in: *Electrochem. Soc. Proc.* **2002-2**, 608 (2002).
15. D. Kot, G. Kissinger, M. A. Schubert, A. Sattler, and T. Müller, *Solid State Phenomena*, **205–206**, 278 (2014).
16. R. J. Falster, V. V. Voronkov, V. Y. Resnick, and M. G. Milvidskii, Proc. High Purity Silicon VIII, ed. by C. Claeys, M. Watanabe, R. Falster, and P. Stallhofer, in: *Electrochem. Soc. Proc.*, **5**, 188 (2004).
17. A. Ourmazd, *Appl. Phys. Lett.*, **45**, 781 (1984).
18. F. Shimura, *Semiconductors and Semimetals*, **42**, 577 (1994).
19. K. Sueoka, S. Ohara, S. Shiba, and S. Fukatani, *ECS Transactions*, **2**, 261 (2006).
20. P. Bai, G. R. Yang, and T. M. Lu, *J. Appl. Phys.*, **68**, 3313 (1990).
21. M. Yonemura, K. Sueoka, and K. Kamei, *J. Appl. Phys.*, **88**, 503 (2000).
22. H. Fukuda, M. Yasuda, and T. Iwabuchi, *Appl. Phys. Lett*, **61**, 693 (1992).
23. T. Yamazaki, Y. Kotaka, and Y. Kataoka, *Ultramicroscopy* **111**, 303 (2011).
24. R. F. Egerton, *Rep. Prog. Phys.*, **72**, 016502 (2009).
25. M. Klingsporn, S. Kirner, C. Villringer, T. Niermann, D. Abou-Ras, I. Costina, M. Lehmann, and B. Stannowski, to be published.
26. T. Malis, S. C. Cheng, and R. F. Egerton, *J. Electron Microscopy Technique*, **8**, 193 (1988).
27. D. Kot, G. Kissinger, M. A. Schubert, and A. Sattler, *ECS Journal of Solid State Science and Technology*, **3**, P370 (2014).
28. P. Moreau, N. Brun, C. A. Walsh, C. Colliex, and A. Howie, *Phys. Rev. B*, **56**, 6774 (1997).
29. M. Couillard, A. Yurtsever, and D. A. Muller, *Phys. Rev. B*, **77**, 085318 (2008).
30. J. Vanhellemont, *J. Appl. Phys.*, **78**, 4297 (1995).
31. O. De Gryse, P. Clauws, J. Van Landuyt, O. Lebedev, C. Claeys, E. Simoen, and J. Vanhellemont, *J. Appl. Phys.*, **91**, 2493 (2002).
32. J. Nicolai, N. Burle, and B. Pichaud, *J. Crystal Growth*, **363**, 93 (2013).
33. A. Borghesi, A. Piaggi, A. Sassella, A. Stella, and B. Pivac, *Phys. Rev. B*, **46**, 4123 (1992).
34. M. Meduňa, O. Caha, and J. Buršík, *J. Cryst. Growth*, **348**, 53 (2012).
35. S. Isomae, H. Ishida, T. Itoga, and K. Hozawa, *J. Electrochem. Soc.*, **149**, G343 (2002).
36. S. M. Myers, M. Seibt, and W. Schröter, *J. Appl. Phys.*, **88**, 3795 (2000).
37. G. Kissinger, D. Kot, M. A. Schubert, A. Sattler, and T. Müller, *Solid State Phenom.*, **242**, 236 (2016).
38. E. R. Weber, *Appl. Phys. A*, **30**, 1 (1983).